Magnetically Induced Topological Evolutions of Exceptional Points in Photonic Bands

Xingqi Zhao,[1] Jiajun Wang,[1,*] Wenzhe Liu,[2] Lei Shi,[1,2,3,4] and Jian Zi[1,2,3,4]

[1]State Key Laboratory of Surface Physics, Key Laboratory of Micro- and Nano-Photonic Structures (Ministry of Education) and Department of Physics, Fudan University, Shanghai 200433, China

[2]Institute for Nanoelectronic Devices and Quantum Computing, Fudan University, Shanghai 200438, China

[3]Collaborative Innovation Center of Advanced Microstructures, Nanjing University, Nanjing 210093, China

[4]Shanghai Research Center for Quantum Sciences, Shanghai 201315, China

(Received 8 January 2025; revised 17 June 2025; accepted 20 June 2025; published 22 July 2025)

Exceptional points (EPs) have been widely studied in various non-Hermitian systems, exhibiting and underlying many unique topological properties. In photonic systems, multiple degrees of freedom of light enable the EPs with rich properties and high dimensional topology. In this Letter, we propose that the external magnetic field can serve as an additional parameter dimension to manipulate EPs with tunable evolutions and hidden topological structures in magneto-optical photonic crystal slabs. Continuous evolution of EPs can be derived by changing the external magnetic field, where paired EPs gradually approach each other as the Fermi arc shrinks, and eventually merge and annihilate. When considering the parameter space including the magnetic field dimension, these EPs form a closed ring, revealing novel topological structures. The discovered EP ring is further associated with more topological polarization properties, including the closed ring in Poincaré sphere and the transferred topological charge between the Fermi arc and the circularly polarized states in momentum space. Our Letter reveals complex topological properties in magneto-optical photonic crystal slabs, providing a framework to explore non-Hermitian topological systems with additional parameter dimensions.

DOI: 10.1103/wv2n-51qg

Degeneracies are fundamental in physical systems, spanning fields from quantum mechanics to classical wave dynamics. In non-Hermitian systems, degeneracies give rise to a unique class of singularities known as exceptional points (EPs) [1–6]. Unlike conventional Hermitian degeneracies, EPs are characterized by the coalescence of both eigenvalues and eigenstates [7], exhibiting unique physical properties. Especially, in photonic systems, EPs have garnered significant attention across various platforms, such as waveguides [8,9], microresonators [10–13], and photonic crystal (PhC) slabs [14–18], due to their promising applications in areas like sensing [19–22], light manipulation [23–25], and nonreciprocal optical devices [26–28]. The topological structures and underlying properties of EPs form the basis for these phenomena, highlighting the critical importance of investigating more intricate and diverse topological configurations.

In the research of topological physics, new degrees of freedom or high-order topological configurations can usually be found by introducing additional parameter dimensions [22,29–33]. For EPs in traditional optical systems, the modulation primarily focused on gain and loss mechanisms. Further exploration of non-Hermitian degeneracies have involved additional parameter dimensions, such as wave vectors, frequency, and phases, leading to the discovery of various EP-related topological configurations, such as higher-order EPs [34,35] and EP lines and rings [36,37]. These developments highlight the critical role of exploring new parameter spaces in uncovering richer non-Hermitian topological phenomena and advancing the understanding of EPs in complex photonic systems.

As periodic structures with open boundaries coupled to free space, PhC slabs support photonic bands in momentum space, where radiation losses are inevitable for leaky optical modes [38]. This intrinsic non-Hermiticity enables Hermitian degeneracies in photonic bands, such as Dirac cones, to evolve into paired EPs or exceptional rings [14–16]. Because of their radiative properties, these EPs in PhC slabs exhibit unique far-field polarization characteristics, closely linked to topological polarization configurations in momentum space [15,16,39]. Beyond the intrinsic degrees of freedom of photonic bands, magnetic fields introduce an additional parametric dimension in the study of topological photonics in magneto-optical (MO) structures, facilitating the emergence of novel topological states [40–43]. Subsequent studies have demonstrated that magnetic fields can generate singular optical modes in MO PhC slabs, further enriching their topological properties when combined with the intrinsic momentum and polarization characteristics of PhC slabs [44–47]. Recently,

*Contact author: jiajunwang@fudan.edu.cn

magnetic fields have been shown to effectively modulate EPs in optical cavity systems, introducing a powerful new dimension for controlling non-Hermitian dynamics [22]. By leveraging the intrinsic polarization and momentum characteristics of PhC slabs, magnetic fields have the potential to unlock unprecedented non-Hermitian phenomena and realize novel topological configurations. However, despite these promising prospects, the role of magnetic field modulation in shaping EPs and the associated topological features in MO PhC slabs remains largely unexplored.

In this Letter, we investigate the magnetically induced topological evolutions of EPs in MO PhC slabs. Starting from paired EPs connected by a Fermi arc in momentum space, we revealed the rich evolutions induced by the magnetic field: as the magnetic field strength increases, the EPs undergo polarization transitions while approaching each other, eventually merging and annihilating with a sufficiently strong magnetic field. This process is accompanied by the transfer of topological charges from the Fermi arc to circularly polarized states (C points), representing a new mechanism for topological charge evolution in momentum space. Moreover, by considering the magnetic field as an additional parameter dimension, we discovered the formation of a closed EP ring, extending the topological structure from the momentum space to a higher-dimensional parameter space. Through the investigation of eigenvalue and polarization evolutions, we demonstrate that magnetic fields can serve as an effective modulation dimension for exploring novel topological configurations and polarization characteristics of non-Hermitian degeneracies in PhC slabs.

We start from the Hermitian case for two-dimensional (2D) PhCs, where the Dirac degeneracies can extensively exist. Here, we take a 2D PhC with square lattice and rectangular holes as an example, shown in the left panel of Fig. 1(a). This structure can support Dirac points located along high-symmetry lines, for example, along the k_x direction. The dispersion around Dirac points can be expressed by a Hamiltonian model in the circular polarization basis [15],

$$H_0 = \begin{pmatrix} 0 & v_x\delta k_x - \mathrm{i}v_y\delta k_y \\ v_x\delta k_x + \mathrm{i}v_y\delta k_y & 0 \end{pmatrix} = v_x\delta k_x\sigma_x + v_y\delta k_y\sigma_y, \quad (1)$$

where v_x and v_y are the two components of group velocities, σ_i $(i = x, y, z)$ is the Pauli matrix, and $\delta\boldsymbol{k} = (\delta k_x, \delta k_y)$ is the wave vector deviates from the Dirac point. This Hamiltonian model gives the linear dispersion around the Dirac point, shown in the left panel of Fig. 1(a).

Different from the 2D PhC, for a PhC slab with finite thickness t [shown in the middle panel of Fig. 1(a)], the optical modes typically become radiative if they are located

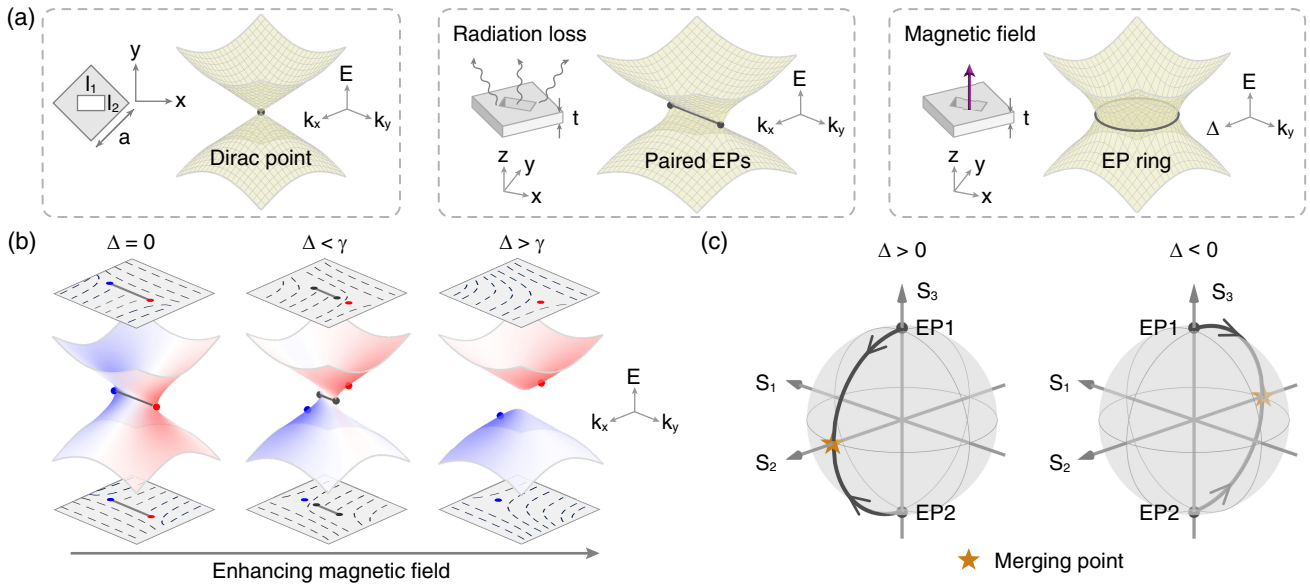

FIG. 1. (a) Left panel: schematic view of a two-dimensional (2D) PhC, which can support Dirac cones with linear dispersion. Middle panel: for a PhC slab, the original Dirac point evolves into a pair of EPs connected by the bulk Fermi arc. Right panel: with an external magnetic field to the MO PhC slab, the EPs form a closed ring with the magnetic field considered as an additional parameter space. (b) Evolutions of EPs and polarization configurations in momentum space with enhancing external magnetic field. Left panel: without the magnetic field, an EP is left-handed circularly polarized (LCP) and the other EP is right-handed circularly polarized (RCP), marked by red and blue dots, respectively. Middle panel: with a weak magnetic field, the bulk Fermi arc shrinks and the EPs are no longer circularly polarized (marked by gray dots), while the circularly polarized states remain and become the vortex centers. Right panel: with a strong magnetic field, the Fermi arc vanishes and EPs do not exist. (c) The evolutions of EPs on the Poincaré sphere with different Δ.

within the light cone. Considering the radiation losses of modes, then the Hamiltonian becomes non-Hermitian and takes the form of [15,16]

$$H = \mathrm{i}\gamma_0 + \mathrm{i}\gamma\sigma_x + v_x\delta k_x\sigma_x + v_y\delta k_y\sigma_y, \tag{2}$$

where γ_0 represents the average decay rate of the modes, and γ characterizes the difference between their decay rates. That is, along the k_x direction, the two orthogonal modes have different decay rates $\gamma_1 = \gamma_0 + \gamma$ and $\gamma_2 = \gamma_0 - \gamma$. The eigenvalues of the Hamiltonian become complex values $\tilde{\omega} = E + \mathrm{i}\Gamma$ (E and Γ are real values). The previous Dirac point in 2D PhC then evolves into a pair of EPs, where the Hamiltonian only has one eigenvalue and eigenstate. From the non-Hermitian Hamiltonian model, the positions of the EPs are $\boldsymbol{k}_{\mathrm{EP}} = (0, \pm\gamma/v_y)$. The paired EPs are linked by a line—the bulk Fermi arc, as shown in the middle panel of Fig. 1(a).

When an external magnetic field is applied perpendicular to the MO PhC slab, the coupling between modes acts as a Zeeman splitting $\Delta\sigma_z$ in the Hamiltonian model [48,49]. Here, Δ represents the coupling strength whose sign is determined by the magnetic field direction and magnitude is controlled by the magnetic field strength. Now, the Hamiltonian model becomes

$$H_{\mathrm{MO}} = \mathrm{i}\gamma_0 + \mathrm{i}\gamma\sigma_x + v_x\delta k_x\sigma_x + v_y\delta k_y\sigma_y + \Delta\sigma_z, \tag{3}$$

and the positions of EPs in momentum space are

$$\boldsymbol{k}_{\mathrm{EP}} = \left(0, \pm\frac{\sqrt{\gamma^2 - \Delta^2}}{v_y}\right). \tag{4}$$

Thus, with increasing $|\Delta|$ (enhancing the external magnetic field), the two EPs become closer, and the length of the Fermi arc shrinks. Eventually, the EPs will merge and annihilate at $|\Delta| = \gamma$. Moreover, with Δ acts as an additional parameter dimension, there will be intriguing topological configurations of EPs. When we fix our attention at $\delta k_x = 0$ and take δk_y and Δ as the parameter space, then the paired EPs will form a ring, governed by

$$v_y^2\delta k_y^2 + \Delta^2 = \gamma^2. \tag{5}$$

This EP ring configuration is shown in the right panel of Fig. 1(a).

For the PhC slab considered, polarization dimensions are inherent in the photonic bands due to the existing far-field radiations of these optical modes, giving rise to topological polarization configurations in momentum space [15,16]. Without the magnetic field ($\Delta = 0$), the eigenstates of EPs are $\psi_{\mathrm{EP}} = (1, 0)^{\mathrm{T}}$ or $(0, 1)^{\mathrm{T}}$, corresponding to circular polarizations in this basis, marked by the red and blue dots in the left panel of Fig. 1(b). Around the bulk Fermi arc for both upper and lower bands, the azimuthal angles of the polarization states wind by $-\pi$, corresponding to a topological charge of $-1/2$. Here, the topological charge of a polarization vortex is defined as [50]

$$q = \frac{1}{2\pi}\oint \mathrm{d}\boldsymbol{k}_{\parallel} \cdot \nabla_{\boldsymbol{k}_{\parallel}}\phi(\boldsymbol{k}_{\parallel}), \tag{6}$$

where $\phi(\boldsymbol{k}_{\parallel})$ is the azimuthal angle of the polarization states' major axis. While with a nonzero external magnetic field, for the case $\Delta < \gamma$, the paired EPs are no longer circularly polarized and marked by gray dots in the middle panel of Fig. 1(b). Here, we focus on the case $\Delta > 0$, while discussions for $\Delta < 0$ are provided in Supplemental Material [51]. For the previous positions the EPs located, on the upper band there is a left-handed circularly polarized (LCP) C point remaining (marked by a red dot), and on the lower band there is a right-handed circularly polarized (RCP) C point remaining (marked by blue dot). The winding angle around the Fermi arc becomes zero, manifesting that the Fermi arc does not carry any topological charge. The $-1/2$ charge is transferred to the C points, as shown in the middle panel of Fig. 1(b). When Δ becomes larger than γ, the EPs annihilate while the C points still exist, and the topological charges are still carried by the C points, as shown in the right panel of Fig. 1(b). For the case $\Delta < 0$, the bands will have similar evolution behavior, while the C points have opposite k_y coordinate and opposite handedness compared to those of $\Delta > 0$. Details are in Supplemental Material [51].

Besides the eigen energy evolutions, with the introduced magnetic dimension, we find the eigen polarizations of EPs will also evolve with the applied magnetic field. In Fig. 1(c), we show the evolution of the EPs' polarizations on the Poincaré sphere with different Δ. With gradual increasing $|\Delta|$, the two EPs transition from the poles of the Poincaré sphere (circular polarizations) to the equator (linear polarization), where they merge and annihilate at a point denoted by a star on the sphere. Different values of Δ drive the EPs' polarization states to form a closed loop on the Poincaré sphere, revealing hidden polarization properties.

To provide a clear example and deepen the understanding of the magnetic modulation of non-Hermitian degeneracies in PhC slabs, we focus on the detailed band structures around the EPs in a specific MO PhC slab. Here, the lattice constant a is set to be 840 nm, the thickness of the slab t is 240 nm, and the length (l_1) and width (l_2) of the rectangular hole are 400 and 100 nm, respectively. The permittivity tensor in the presence of the magnetic field is [52,55]

$$\overleftrightarrow{\varepsilon}_r = \begin{pmatrix} \varepsilon & \mathrm{i}\delta & 0 \\ -\mathrm{i}\delta & \varepsilon & 0 \\ 0 & 0 & \varepsilon \end{pmatrix}, \tag{7}$$

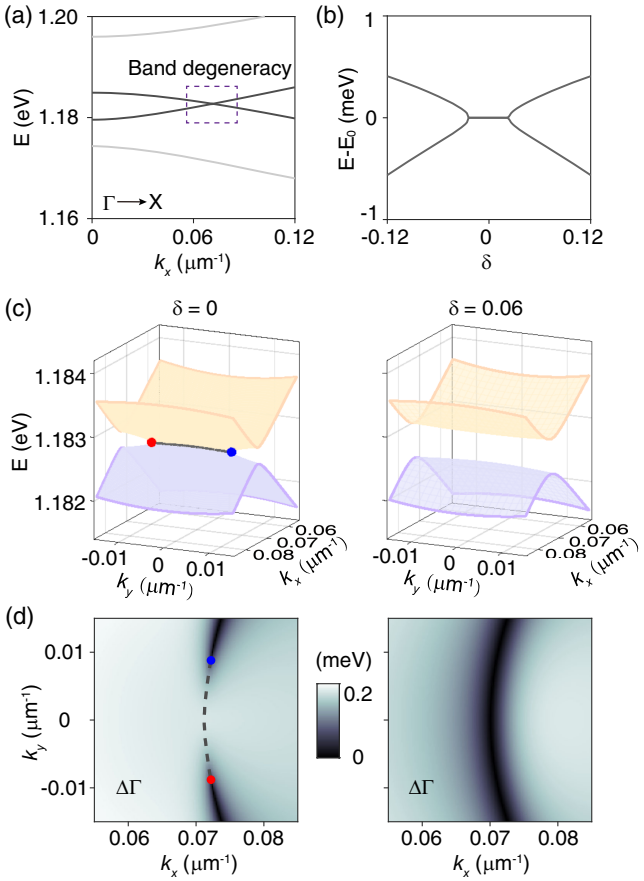

FIG. 2. (a) The dispersion of modes along the k_x direction. The dashed box denotes the band degeneracy of concern. (b) The real part of the energy of modes with different values of δ, i.e., different strengths of external magnetic field. The mean value of the real part of the energy is subtracted. (c) The real part of the energy of modes in the momentum space with $\delta = 0$ (left panel) and $\delta = 0.06$ (right panel). Red and blue dots denote the circularly polarized EPs and the black line denotes the bulk Fermi arc. (d) The difference of the imaginary part of energy between two bands in the momentum space with $\delta = 0$ (left panel) and $\delta = 0.06$ (right panel).

where ε is the permittivity of the material without magnetization, and it is set to be 4 in our calculation. The off-diagonal term δ is the MO parameter, which can be controlled by the external magnetic field strength. In this PhC slab, a band degeneracy can be found along the k_x direction with $\delta = 0$ at $k_x = 0.071$ μm^{-1}, where Fig. 2(a) shows the real part (E) of the modes' eigenvalues.

Figure 2(b) is focusing on the evolution of the real parts of modes' energies at $k_x = 0.071$ μm^{-1}. The mean value of the real part of the energy is subtracted for better visualization. When the magnetic field is applied, the real part of modes still degenerate with a small δ, corresponding to the case $\Delta < \gamma$. With a sufficient strong magnetic field ($\delta > 0.024$), Δ becomes larger than γ and the degeneracy is lifted. For an external magnetic field of opposite direction, i.e., negative δ, the phenomenon is similar to the case of positive δ.

For further illustrating the impact of the magnetic field on modes' eigenvalues, we examine the band structures in momentum space for two specific cases: $\delta = 0$ and 0.06. With $\delta = 0$, the real part of modes is degenerate along a line, i.e., the bulk Fermi arc, as shown in the left panel of Fig. 2(c). Besides, the left panel of Fig. 2(d) exhibits the difference of the imaginary parts of modes' energies ($\Delta\Gamma$). At the paired EPs, which are marked by red and blue dots, both the real part and imaginary part of eigenvalues of modes coalesce. While with $\delta = 0.06$, real parts of two bands are separate, and EPs do not exist. For other values of δ, the detailed evolution of band structures are provided in Supplemental Material [51], showing the shrinking of bulk Fermi arc and merging of EPs.

To exhibit the EPs' evolution in the additional magnetic dimension, we then show the band structures in the $k_y - \delta$ space. In our calculation, the k_x is selected near the EPs as an approximate position to the Fermi arc. Here, Fig. 3(a) depicts the real part of the eigenvalues E for two bands, where the evolution of EPs is denoted as a continuous black curve in the $k_y - \delta$ plane. And Fig. 3(b) shows the corresponding imaginary parts Γ. The simulated eigenvalues directly demonstrate the closed EP ring in the parameter space with the consideration of magnetic field dimension. This new topological configuration makes the MO PhC slab a promising platform for high-sensitivity magneto-optical detection in integrated photonic systems.

Figure 4 shows the evolution of modes' polarization distribution in momentum space as δ increases. The degree of circular polarization of a mode (S_3/S_0) is represented by the background color. Without the external magnetic field, one EP is LCP and the other is RCP. When encircling the Fermi arc, the polarization states wind by $-\pi$ on both bands, corresponding to a topological charge of $-1/2$. Then, with $\delta = 0.020$, for this case Δ is smaller than γ. The EPs still exist, while their polarization states are not circularly polarized. On the upper band, an LCP C point remains, and on the lower band, an RCP C point remains. These C points are characterized by the degree of circular polarization approaching ± 1. As δ increases, the Fermi arc

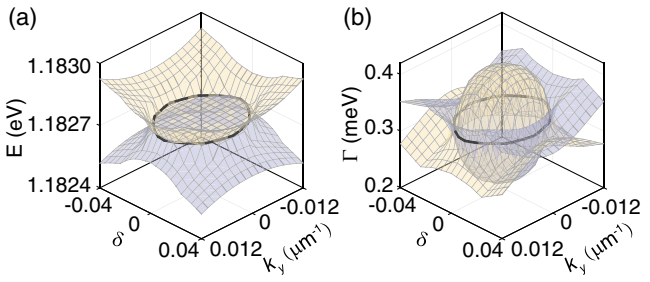

FIG. 3. Calculated results for the EP ring in the $k_y - \delta$ space. (a),(b) The real (imaginary) parts of the two bands' eigenvalues. The EP ring is denoted by the black curve.

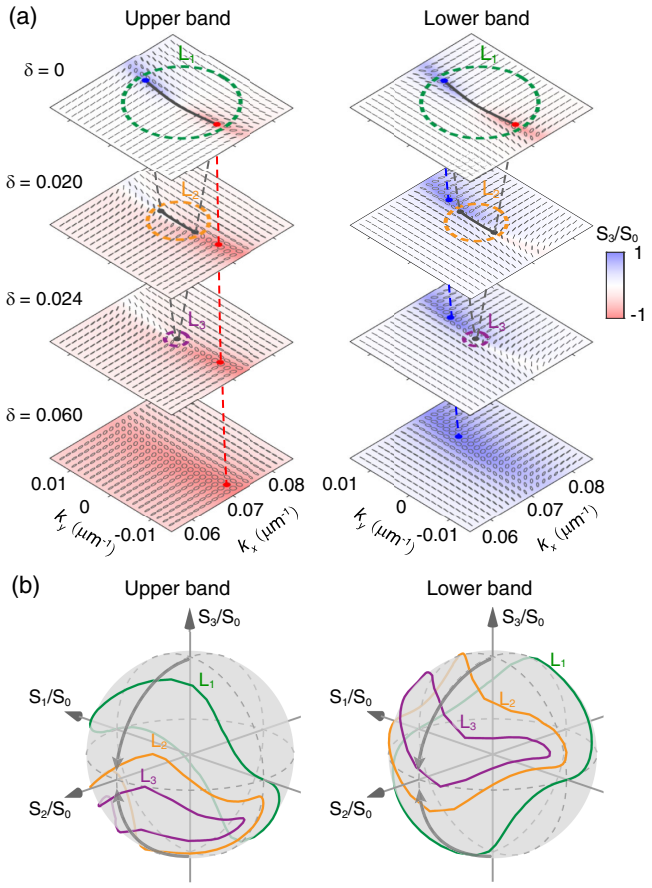

FIG. 4. (a) Evolutions of the polarization distribution in the momentum space with different values of δ. The red and blue dots represent the circularly polarized EPs or C points. The gray dots represent the EPs with nonzero magnetic fields. (b) The polarization states on a closed line around the EPs. The polarization states are represented by the Stokes parameters, projected on the Poincaré sphere.

shrinks and the two EPs eventually merge and then annihilate at $\delta = 0.024$. With increasing δ, for the upper (lower) band, there will be an enlarged area with a high degree of left-(right-)handed circular polarization. With the nonzero δ, the Fermi arc does not carry any topological charge, and the $-1/2$ charge is transferred to the C point.

The polarization properties around the Fermi arc can be directly represented on the Poincaré sphere; Fig. 4(b) shows the polarization states along closed loops encircling the EPs. The chosen loops are marked by L_1, L_2, and L_3 in Fig. 4. On L_1, the polarization states encircle the S_3 axis for one circle, demonstrating that their azimuthal angles wind by $-\pi$. In contrast, for L_2 and L_3, they do not enclose the S_3 axis, indicating that the Fermi arc carries no topological charge. The gray arrows on the Poincaré sphere show the evolution of the EPs, which evolve from circularly polarized to linearly polarized as the δ increases.

To conclude, we have investigated the magnetic modulation of non-Hermitian degeneracies in MO PhC slabs. Through systematic investigation of eigenvalue and polarization evolutions, we revealed how magnetic fields drive the continuous transformation of EPs: the paired EPs gradually approach each other as the Fermi arc shrinks, eventually merging and annihilating at a critical field strength. In the magnetic field parameter space, these EPs form a closed ring, extending the topological structure beyond momentum space. Furthermore, we uncovered the topological charges originally carried by the Fermi arc are transferred to C points under magnetic modulation in the momentum space. These findings not only reveal novel topological configurations and polarization evolution behaviors of non-Hermitian degeneracies under magnetic control but also establish MO photonic devices as a promising platform for exploring and utilizing non-Hermitian topology.

Acknowledgments—This work is supported by National Natural Science Foundation of China (No. 12404427, No. 12234007, No. 124B2084, No. 12321161645, No. 12221004, No. T2394480, and No. T2394481); National Key R&D Program of China (2023YFA1406900 and 2022YFA1404800); Science and Technology Commission of Shanghai Municipality (24YF2702400, 22142200400, 21DZ1101500, 2019SHZDZX01, and 23DZ2260100). J. W. was also supported by the China National Postdoctoral Program for Innovative Talents (BX20230079) and the China Postdoctoral Science Foundation (2023M740721).

X. Z. and J. W. contributed equally to this study.

Data availability—The data that support the findings of this Letter are openly available [56].

[1] R. El-Ganainy, K. G. Makris, M. Khajavikhan, Z. H. Musslimani, S. Rotter, and D. N. Christodoulides, Non-Hermitian physics and PT symmetry, Nat. Phys. **14**, 11 (2018).
[2] M.-A. Miri and A. Alu, Exceptional points in optics and photonics, Science **363**, eaar7709 (2019).
[3] Ş. K. Özdemir, S. Rotter, F. Nori, and L. Yang, Parity–time symmetry and exceptional points in photonics, Nat. Mater. **18**, 783 (2019).
[4] Y. Ashida, Z. Gong, and M. Ueda, Non-Hermitian physics, Adv. Phys. **69**, 249 (2020).
[5] E. J. Bergholtz, J. C. Budich, and F. K. Kunst, Exceptional topology of non-Hermitian systems, Rev. Mod. Phys. **93**, 015005 (2021).
[6] A. Li, H. Wei, M. Cotrufo, W. Chen, S. Mann, X. Ni, B. Xu, J. Chen, J. Wang, S. Fan *et al.*, Exceptional points and non-Hermitian photonics at the nanoscale, Nat. Nanotechnol. **18**, 706 (2023).
[7] W. D. Heiss, The physics of exceptional points, J. Phys. A **45**, 444016 (2012).

[8] J. Doppler, A. A. Mailybaev, J. Böhm, U. Kuhl, A. Girschik, F. Libisch, T. J. Milburn, P. Rabl, N. Moiseyev, and S. Rotter, Dynamically encircling an exceptional point for asymmetric mode switching, Nature (London) **537**, 76 (2016).

[9] X. Shu, A. Li, G. Hu, J. Wang, A. Alù, and L. Chen, Fast encirclement of an exceptional point for highly efficient and compact chiral mode converters, Nat. Commun. **13**, 2123 (2022).

[10] B. Peng, Ş. K. Özdemir, F. Lei, F. Monifi, M. Gianfreda, G. L. Long, S. Fan, F. Nori, C. M. Bender, and L. Yang, Parity–time-symmetric whispering-gallery microcavities, Nat. Phys. **10**, 394 (2014).

[11] H. Hodaei, M.-A. Miri, M. Heinrich, D. N. Christodoulides, and M. Khajavikhan, Parity-time–symmetric microring lasers, Science **346**, 975 (2014).

[12] H. Zhang, R. Huang, S.-D. Zhang, Y. Li, C.-W. Qiu, F. Nori, and H. Jing, Breaking anti-PT symmetry by spinning a resonator, Nano Lett. **20**, 7594 (2020).

[13] C. Wang, W. R. Sweeney, A. D. Stone, and L. Yang, Coherent perfect absorption at an exceptional point, Science **373**, 1261 (2021).

[14] B. Zhen, C. W. Hsu, Y. Igarashi, L. Lu, I. Kaminer, A. Pick, S.-L. Chua, J. D. Joannopoulos, and M. Soljačić, Spawning rings of exceptional points out of dirac cones, Nature (London) **525**, 354 (2015).

[15] H. Zhou, C. Peng, Y. Yoon, C. W. Hsu, K. A. Nelson, L. Fu, J. D. Joannopoulos, M. Soljačić, and B. Zhen, Observation of bulk Fermi arc and polarization half charge from paired exceptional points, Science **359**, 1009 (2018).

[16] W. Chen, Q. Yang, Y. Chen, and W. Liu, Evolution and global charge conservation for polarization singularities emerging from non-hermitian degeneracies, Proc. Natl. Acad. Sci. U.S.A. **118**, e2019578118 (2021).

[17] L. Ferrier, P. Bouteyre, A. Pick, S. Cueff, N. H. M. Dang, C. Diederichs, A. Belarouci, T. Benyattou, J. X. Zhao, R. Su *et al.*, Unveiling the enhancement of spontaneous emission at exceptional points, Phys. Rev. Lett. **129**, 083602 (2022).

[18] X. Yin, T. Inoue, C. Peng, and S. Noda, Topological unidirectional guided resonances emerged from interband coupling, Phys. Rev. Lett. **130**, 056401 (2023).

[19] H. Hodaei, A. U. Hassan, S. Wittek, H. Garcia-Gracia, R. El-Ganainy, D. N. Christodoulides, and M. Khajavikhan, Enhanced sensitivity at higher-order exceptional points, Nature (London) **548**, 187 (2017).

[20] W. Chen, Ş. Kaya Özdemir, G. Zhao, J. Wiersig, and L. Yang, Exceptional points enhance sensing in an optical microcavity, Nature (London) **548**, 192 (2017).

[21] J.-H. Park, A. Ndao, W. Cai, L. Hsu, A. Kodigala, T. Lepetit, Y.-H. Lo, and B. Kanté, Symmetry-breaking-induced plasmonic exceptional points and nanoscale sensing, Nat. Phys. **16**, 462 (2020).

[22] Y.-P. Ruan, J.-S. Tang, Z. Li, H. Wu, W. Zhou, L. Xiao, J. Chen, S.-J. Ge, W. Hu, H. Zhang *et al.*, Observation of loss-enhanced magneto-optical effect, Nat. Photonics **19**, 109–115 (2025).

[23] Q. Song, M. Odeh, J. Zúñiga-Pérez, B. Kanté, and P. Genevet, Plasmonic topological metasurface by encircling an exceptional point, Science **373**, 1133 (2021).

[24] S. Xia, D. Kaltsas, D. Song, I. Komis, J. Xu, A. Szameit, H. Buljan, K. G. Makris, and Z. Chen, Nonlinear tuning of PT symmetry and non-Hermitian topological states, Science **372**, 72 (2021).

[25] Z. Yang, P.-S. Huang, Y.-T. Lin, H. Qin, J. Zúñiga-Pérez, Y. Shi, Z. Wang, X. Cheng, M.-C. Tang, S. Han *et al.*, Creating pairs of exceptional points for arbitrary polarization control: Asymmetric vectorial wavefront modulation, Nat. Commun. **15**, 232 (2024).

[26] L. Feng, M. Ayache, J. Huang, Y.-L. Xu, M.-H. Lu, Y.-F. Chen, Y. Fainman, and A. Scherer, Nonreciprocal light propagation in a silicon photonic circuit, Science **333**, 729 (2011).

[27] Y. Shi, Z. Yu, and S. Fan, Limitations of nonlinear optical isolators due to dynamic reciprocity, Nat. Photonics **9**, 388 (2015).

[28] Y. Choi, C. Hahn, J. W. Yoon, S. H. Song, and P. Berini, Extremely broadband, on-chip optical nonreciprocity enabled by mimicking nonlinear anti-adiabatic quantum jumps near exceptional points, Nat. Commun. **8**, 14154 (2017).

[29] A. Tuniz, T. Wieduwilt, and M. A. Schmidt, Tuning the effective pt phase of plasmonic eigenmodes, Phys. Rev. Lett. **123**, 213903 (2019).

[30] Y. Li, Y.-G. Peng, L. Han, M.-A. Miri, W. Li, M. Xiao, X.-F. Zhu, J. Zhao, A. Alù, S. Fan *et al.*, Anti–parity-time symmetry in diffusive systems, Science **364**, 170 (2019).

[31] Z. Ren, D. Liu, E. Zhao, C. He, K. K. Pak, J. Li, and G.-B. Jo, Chiral control of quantum states in non-Hermitian spin–orbit-coupled fermions, Nat. Phys. **18**, 385 (2022).

[32] L. Yu, H. Xue, R. Guo, E. A. Chan, Y. Y. Terh, C. Soci, B. Zhang, and Y. Chong, Dirac mass induced by optical gain and loss, Nature (London) **632**, 63 (2024).

[33] M. Reisenbauer, H. Rudolph, L. Egyed, K. Hornberger, A. V. Zasedatelev, M. Abuzarli, B. A. Stickler, and U. Delić, Non-Hermitian dynamics and non-reciprocity of optically coupled nanoparticles, Nat. Phys. **20**, 1629 (2024).

[34] S. Wang, B. Hou, W. Lu, Y. Chen, Z. Zhang, and C. T. Chan, Arbitrary order exceptional point induced by photonic spin–orbit interaction in coupled resonators, Nat. Commun. **10**, 832 (2019).

[35] Q. Zhong, J. Kou, Ş. K. Özdemir, and R. El-Ganainy, Hierarchical construction of higher-order exceptional points, Phys. Rev. Lett. **125**, 203602 (2020).

[36] A. Cerjan, S. Huang, M. Wang, K. P. Chen, Y. Chong, and M. C. Rechtsman, Experimental realization of a Weyl exceptional ring, Nat. Photonics **13**, 623 (2019).

[37] Y. S. Patil, J. Höller, P. A. Henry, C. Guria, Y. Zhang, L. Jiang, N. Kralj, N. Read, and J. G. Harris, Measuring the knot of non-Hermitian degeneracies and non-commuting braids, Nature (London) **607**, 271 (2022).

[38] L. Huang, L. Xu, D. A. Powell, W. J. Padilla, and A. E. Miroshnichenko, Resonant leaky modes in all-dielectric metasystems: Fundamentals and applications, Phys. Rep. **1008**, 1 (2023).

[39] A. Chen, W. Liu, Y. Zhang, B. Wang, X. Liu, L. Shi, L. Lu, and J. Zi, Observing vortex polarization singularities at optical band degeneracies, Phys. Rev. B **99**, 180101(R) (2019).

[40] Z. Wang, Y. D. Chong, J. D. Joannopoulos, and M. Soljačić, Reflection-free one-way edge modes in a gyromagnetic photonic crystal, Phys. Rev. Lett. **100**, 013905 (2008).
[41] Z. Wang, Y. Chong, J. D. Joannopoulos, and M. Soljačić, Observation of unidirectional backscattering-immune topological electromagnetic states, Nature (London) **461**, 772 (2009).
[42] L. Lu, J. D. Joannopoulos, and M. Soljačić, Topological photonics, Nat. Photonics **8**, 821 (2014).
[43] T. Ozawa, H. M. Price, A. Amo, N. Goldman, M. Hafezi, L. Lu, M. C. Rechtsman, D. Schuster, J. Simon, O. Zilberberg *et al.*, Topological photonics, Rev. Mod. Phys. **91**, 015006 (2019).
[44] C. Zhao, S. Dong, Q. Zhang, Y. Zeng, G. Hu, and Y. Zhang, Magnetic modulation of topological polarization singularities in momentum space, Opt. Lett. **47**, 2754 (2022).
[45] X. Zhao, J. Wang, W. Liu, Z. Che, X. Wang, C. T. Chan, L. Shi, and J. Zi, Spin-orbit-locking chiral bound states in the continuum, Phys. Rev. Lett. **133**, 036201 (2024).
[46] Q.-A. Tu, H. Zhou, D. Zhao, Y. Meng, M. Gong, and Z. Gao, Magnetically tunable bound states in the continuum with arbitrary polarization and intrinsic chirality, Photonics Res. **12**, 2972 (2024).
[47] W. Lv, H. Qin, Z. Su, C. Zhang, J. Huang, Y. Shi, B. Li, P. Genevet, and Q. Song, Robust generation of intrinsic C points with magneto-optical bound states in the continuum, Sci. Adv. **10**, eads0157 (2024).
[48] F. D. M. Haldane and S. Raghu, Possible realization of directional optical waveguides in photonic crystals with broken time-reversal symmetry, Phys. Rev. Lett. **100**, 013904 (2008).
[49] S. Raghu and F. D. M. Haldane, Analogs of quantum-Hall-effect edge states in photonic crystals, Phys. Rev. A **78**, 033834 (2008).
[50] M. Kang, T. Liu, C. Chan, and M. Xiao, Applications of bound states in the continuum in photonics, Nat. Rev. Phys. **5**, 659 (2023).
[51] See Supplemental Material at http://link.aps.org/supplemental/10.1103/wv2n-51qg for details of the eigenstates of the Hamiltonian model, the polarization distribution from the Hamiltonian model, the simulated evolutions of band structures with different external magnetic field, and other related discussions, which includes Refs. [15,16,22,52–54].
[52] K. J. Buschow, *Handbook of Magnetic Materials* (Elsevier, Amsterdam, 2003).
[53] J. Chin, T. Steinle, T. Wehlus, D. Dregely, T. Weiss, V. Belotelov, B. Stritzker, and H. Giessen, Nonreciprocal plasmonics enables giant enhancement of thin-film faraday rotation, Nat. Commun. **4**, 1599 (2013).
[54] Y. Yang, Y. Liu, J. Qin, S. Cai, J. Su, P. Zhou, L. Deng, Y. Li, and L. Bi, Magnetically tunable zero-index metamaterials, Photonics Res. **11**, 1613 (2023).
[55] T. Haider, A review of magneto-optic effects and its application, Int. J. Electromagn. Appl **7**, 17 (2017).
[56] X. Zhao, Plotting data for figures in the paper "Magnetically Induced Topological Evolutions of Exceptional Points in Photonic Bands", 10.5281/zenodo.15744537.